J|A|C|S ARTICLES

Published on Web 03/10/2010

# Reactions of the Terminal $Ni^{II}$−OH Group in Substitution and Electrophilic Reactions with Carbon Dioxide and Other Substrates: Structural Definition of Binding Modes in an Intramolecular $Ni^{II}\cdots Fe^{II}$ Bridged Site

Deguang Huang and R. H. Holm*

*Department of Chemistry and Chemical Biology, Harvard University, Cambridge, Massachusetts 02138*

Received January 13, 2010; E-mail: holm@chemistry.harvard.edu

***Abstract:*** A singular feature of the catalytic C-cluster of carbon monoxide dehydrogenase is a sulfide-bridged Ni···Fe locus where substrate is bound and transformed in the reversible reaction $CO + H_2O \rightleftharpoons CO_2 + 2H^+ + 2e^-$. A similar structure has been sought in this work. Mononuclear planar $Ni^{II}$ complexes $[Ni(pyN_2^{Me2})L]^{1-}$ ($pyN_2^{Me2}$ = bis(2,6-dimethylphenyl)-2,6-pyridinedicarboxamidate(2−)) derived from a NNN pincer ligand have been prepared including $L = OH^-$ (**1**) and $CN^-$ (**7**). Complex **1** reacts with ethyl formate and $CO_2$ to form unidentate $L = HCO_2^-$ (**5**) and $HCO_3^-$ (**6**) products. A binucleating macrocycle was prepared which specifically binds $Ni^{II}$ at a NNN pincer site and five-coordinate $Fe^{II}$ at a triamine site. The $Ni^{II}$ macrocyle forms hydroxo (**14**) and cyanide complexes (**15**) analogous to **1** and **7**. Reaction of **14** with $FeCl_2$ alone and with ethyl formate and **15** with $FeCl_2$ affords molecules with the $Ni^{II}$−L−$Fe^{II}$ bridge unit in which L = $\mu_2$:$\eta^1$-$OH^-$ (**17**) and $\mu_2$:$\eta^2$-$HCO_2^-$ (**18**) and $-CN^-$ (**19**). All bridges are nonlinear (**17**, 140.0°; **18**, M−O−C 135.9° (Ni), 120.2° (Fe); **19**, Ni−C−N 170.3°, Fe−N−C 141.8°) with Ni···Fe separations of 3.7−4.8 Å. The $Ni^{II}Fe^{II}$ complexes, lacking appropriate Ni−Fe−S cluster structures, are not site analogues, but their synthesis and reactivity provide the first demonstration that molecular $Ni^{II}\cdots Fe^{II}$ sites and bridges can be attained, a necessity in the biomimetic chemistry of C-clusters.

## Introduction

Among the many challenges in the biomimetic chemistry of metal clusters[1] is the construction of molecules that approach or achieve the structures of the catalytic sites of carbon monoxide dehydrogenases (CODHs[2]).[3,4] These enzymes contain either a Mo−Cu−S or a Ni−Fe−S active site and catalyze the reversible reaction $CO + H_2O \rightleftharpoons CO_2 + 2H^+ + 2e^-$, a process of prime significance in the global carbon cycle. Nickel-containing CODHs[5,6] utilize as their catalytic site for $CO/CO_2$ interconversion the structurally complex C-cluster, which has been crystallographically investigated in enzymes from several different anaerobic bacteria.[7−9] The most recent results (2007−09) for enzymes from three sources (*Mt*CODH,[10] *Mb*CODH/ACS,[11] *Mt*CODH/ACS[12]) point toward a consistent structure based on a $NiFe_3S_4$ cluster to which is appended an external (exo) iron atom. As shown in Figure 1 (a), the structure is a bridged assembly of core composition $NiFe_4S_4$ with an aquo or hydroxo ligand bound to the exo iron with approximate tetrahedral geometry. The consensus structure-based mechanistic proposal is that CO binds at the nickel site, undergoes nucleophilic attack by coordinated hydroxide to form a carbon-bound hydroxycarbonyl bridged intermediate such as (b). This species subsequently liberates $CO_2$ and two electrons upon reaction with water to regenerate (a).

Previous synthetic work directed toward the C-cluster, some of it prior to the availability of structural information, has resulted in clusters with certain relevant features. Phosphine ligation in the cubanes $[(Ph_3P)NiFe_3S_4(SR)_3]^{2-}$ simulates the binding of CO and other $\pi$-acid ligands at a tetrahedral nickel site.[13−15] Further, the approximately planar Ni sites in intermediate (b) and the cyanide-ligated C-clusters (c) and (d) (Figure 1) are approached in clusters such as $[(tdt)NiFe_3S_4(LS_3)]^{3-}$. This and related cubanoid clusters are produced by phosphine substitution with a strong in-plane chelating ligand and attendant

(1) Groysman, S.; Holm, R. H. *Biochemistry* **2009**, *48*, 2310–2320.
(2) Abbreviations are given in Chart 1.
(3) Ragsdale, S. W.; Kumar, M. *Chem. Rev.* **1996**, *96*, 2515–2539.
(4) Ragsdale, S. W. *Crit. Rev. Biochem. Mol. Biol.* **2004**, *39*, 165–195.
(5) Lindahl, P. A. *Biochemistry* **2002**, *41*, 2097–2105.
(6) Lindahl, P. A.; Graham, D. E. *Metal Ions Life Sci.* **2007**, *2*, 357–415.
(7) Drennan, C. L.; Doukov, T. I.; Ragsdale, S. W. *J. Biol. Inorg. Chem.* **2004**, *9*, 511–515.
(8) Dobbek, H.; Svetlitchnyi, V.; Liss, J.; Meyer, O. *J. Am. Chem. Soc.* **2004**, *126*, 5382–5387.
(9) Volbeda, A.; Fontecilla-Camps, J. C. *J. Chem. Soc., Dalton Trans.* **2005**, 3443–3450.
(10) Jeoung, J.-H.; Dobbek, H. *Science* **2007**, *318*, 1461–1464.
(11) Gong, W.; Hao, B.; Wei, Z.; Ferguson, D. J.; Tallant, T.; Krzycki, J. A.; Chan, M. K. *Proc. Natl. Acad. Sci. U.S.A.* **2008**, *105*, 9558–9563.
(12) Kung, Y.; Doukov, T. I.; Seravalli, J.; Ragsdale, S. W.; Drennan, C. L. *Biochemistry* **2009**, *48*, 7432–7440.
(13) Ciurli, S.; Ross, P. K.; Scott, M. J.; Yu, S.-B.; Holm, R. H. *J. Am. Chem. Soc.* **1992**, *114*, 5415–5423.
(14) Zhou, J.; Scott, M. J.; Hu, Z.; Peng, G.; Münck, E.; Holm, R. H. *J. Am. Chem. Soc.* **1992**, *114*, 10843–10854.
(15) Zhou, J.; Raebiger, J. W.; Crawford, C. A.; Holm, R. H. *J. Am. Chem. Soc.* **1997**, *119*, 6242–6250.

 © 2010 American Chemical Society 

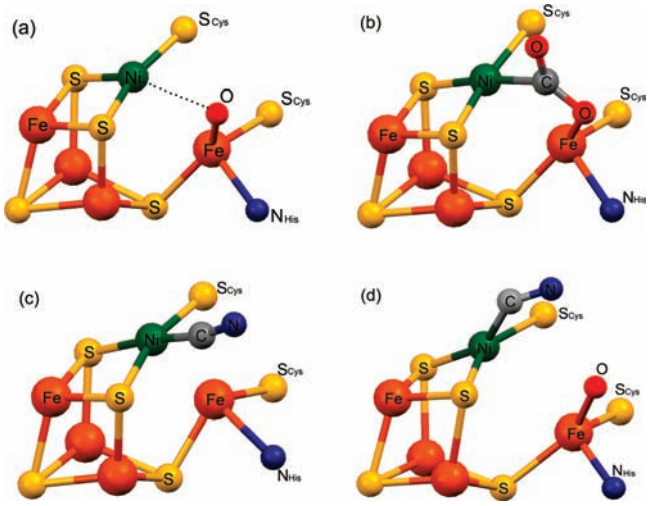


***Figure 1.*** Structures of C-clusters in different reaction states with selected interatomic distances (Å) and angles. (a) *Ch*CODH in the $C_{red1}$ or −320 mV (resting) state: Ni−O, 2.72; Fe−O, 1.95; Ni−Fe, 2.85.[10] (b) *Ch*CODH in the −600 + $CO_2$ (intermediate) state: Ni−C, 1.96; Fe−O, 2.05; $C-O_{Fe}$, 1.25; Ni−Fe, 2.76; Ni−C−O, 119°; Fe−O−C, 105°.[10] (c) *Ch*CODH in the cyanide-bound state: Ni−C, 1.79; Ni−Fe, 2.56; Ni−C−N, 170°.[10] (d) *Mt*CODH/ACS in the cyanide-bound state: Ni−C, 1.99; Fe−O, 2.05; Ni−C−N, 114°.[12] In (a) and (d), $OH^-/OH_2$ is bound to Fe. Terminal cysteinate ligation at three Fe atoms in each structure is omitted.

rupture of the axial Ni−($\mu_3$-S) bond.[16,17] However, key attributes of the C-cluster have not been experimentally attained. These include an exo iron site linked to the $NiFe_3S_4$ portion through a $\mu_3$-S bridge (or any bridge), coordinative unsaturation at the nickel site as manifested in the apparent three-coordinate "T-shaped"[10] Ni($\mu_3$-S)$_2S_{Cys}$ fragment (Figure 1 (a)) and the juxtaposition of a terminal $OH^-/OH_2$ ligand at a distance too long to represent a bridging interaction to the nickel site (Ni···OH 2.7 Å). Multiple attempts to bridge $Fe^{II}$ to an $NiFe_3S_4$ unit have not succeeded.

Given the current synthetic inaccessibility of a complete C-cluster analogue, we have utilized a different ligand construct with which to pursue reactivity with CO and $CO_2$ by $Ni^{II}$ alone and in the presence of proximal $Fe^{II}$. The few terminal $Fe^{II}$−OH complexes known are stabilized by steric factors[18] or hydrogen-bonding interactions;[19,20] reactivity toward CO or $CO_2$ has not been reported. Pincer $Ni^{II}$, $Pd^{II}$, and $Pt^{II}$ terminal hydroxo complexes with PCP donor atom sets react with these substrates, in several cases affording C-bound hydroxycarbonyl products[21−23] similar to intermediate (b) but bound in the $\eta^1$ mode. Consequently, we have utilized pincers with a less-abiological NNN donor set as a ligand for $Ni^{II}$ in mononuclear complexes and in a binucleating macrocycle incorporating a triamine (dien) binding site for $Fe^{II}$. This investigation is an initial step toward a binuclear $Ni^{II}$···$Fe^{II}$ system allowing examination of biological substrate and inhibitor binding at one or both metal centers in terminal or bridge modes. Other than with the enzymes themselves, there is no information on reactivity and structures of binuclear $Ni^{II}Fe^{II}$ molecules with any species.

## Experimental Section

**Preparation of Compounds.** All reactions and manipulations were performed under a pure dinitrogen atmosphere using Schlenk techniques or an inert atmosphere box. Volume reduction and drying steps were performed in vacuo. DMF was freshly distilled and dried over 3-Å molecular sieves for 3 d. Other solvents were passed through an Innovative Technology or MBraun solvent purification system. All solvents were degassed before use. Compounds were identified by spectroscopic and/or crystallographic characterization; representative compounds were analyzed (Kolbe Microanalytical Laboratory, Mülheim, Germany). Cation resonances are omitted from NMR data. Compounds with no NMR data were insufficiently soluble for measurement and were identified crystallographically.

In the sections that follow, complexes and ligands are numerically designated according to Chart 1.

***Chart 1.*** Abbreviations and Designation of Ligands and Complexes[a]

| | |
|---|---|
| $[Ni(pyN_2^{Me2})L]^{1-}$ | L = $OH^-$ **1**, $Cl^-$ **2**, $OMe^-$ **3**, $SH^-$ **4** |
| | $HCO_2^-$ **5**, $HCO_3^-$ **6**, $CN^-$ **7** |
| $[Ni(pyN_2^{Me2})(CN)Fe(Me_6tren)]^{1+}$ | **8** |
| macrocycle intermediates | **9-12** |
| ⊂-$H_2pyN_2dien^{Me3}$ | **13** |
| $[Ni(L)(⊂\text{-}pyN_2dien^{Me3})]^{1-}$ | L = $OH^-$ **14**, $CN^-$ **15**, $HCO_3^-$ **16** |
| $[Ni(L)FeCl(⊂\text{-}pyN_2dien^{Me3})]$ | L = $OH^-$ **17**, $HCO_2^-$ **18**, $CN^-$ **19** |
| $[Pd(pyN_2^{Me2})L]^{1-}$ | L = $OH^-$ **20**, $HCO_3^-$ **21** |

[a] ACS = acetyl coenzyme A synthase; *Ch* = *Carboxydothermus hydrogenoformans*; CODH = carbon monoxide dehydrogenase; dien = diethylenetriamine; dme = 1,2-dimethoxyethane; *Mb* = *Methanosarcina barkeri*; $Me_6$tren = tris(*N*,*N*′-dimethyl-2-aminoethyl)amine; *Mt* = *Moorella thermoacetica;* $pyN_2$ = *N*,*N*′-bis(phenyl)-2,6-pyridinedicarboxamidate(2-); pdtc = pyridine-2,6-dithiocarboxylate(2−); $pyN_2^{iPr2}$ = *N*,*N*′-bis(2,6-diisopropylphenyl)-2,6-pyridinedicarboxamidate(2−); $pyN_2^{Me2}$ = bis(2,6-dimethylphenyl)-2,6-pyridinedicarboxamidate(2−); $pyN_2dien^{Me3}$ = bis(phenyl-3,3′-(2,5,8-tri-*N*-methylamino-1,9-nonyl))-2,6-pyridinedicarboxamidate(2−); tdt = toluene-3,4-dithiolate(2−); $TfO^-$ = triflate.

**(a) Pincer Ligand and Mononuclear Complexes. *N*,*N*′-Bis(2,6-dimethylphenyl)-2,6-pyridinedicarboxamide ($H_2pyN_2^{Me2}$).** A solution of pyridine-2,6-dicarbonyl chloride (1.02 g, 5.00 mmol) at 0 °C in THF (150 mL) was added slowly to a mixture of 2,6-dimethylaniline (1.21 g, 10 mmol) and triethylamine (1.41 mL, 10 mmol). The reaction mixture was warmed to room temperature, stirred for 5 h, and filtered. The light yellow residue obtained by removal of solvent was treated with hexane (10 mL) and washed with a small volume of dichloromethane/ether (1:5 v/v) to give the pure product as a white powder (1.58 g, 85%). $^1$H NMR ($CDCl_3$): $\delta$ 2.27 (s, 12), 7.13 (m, 6), 8.14 (t, 1), 8.51 (d, 2) 9.17 (s, 2).

Synthetic reactions for complexes are summarized in Figure 2.

**($Et_4N$)[$Ni(pyN_2^{Me2})(OH)$].** $H_2pyN_2^{Me2}$ (149 mg, 0.40 mmol) and $Ni(OTf)_2$ (143 mg, 0.40 mmol) were stirred in THF (5 mL) for 2 h. The light yellow suspension was treated with $Et_4NOH$ (25% in methanol, 353 mg, 0.60 mmol) and stirred for 2 h to give a red suspension. A second equal portion of $Et_4NOH$ was added, and the mixture was stirred for 10 h to afford a deep red solution and some sticky precipitate, which was removed by filtration through Celite. Hexane (10 mL) was added to the filtrate resulting in separation of a red oil. Addition of ether (5 mL) to the oil resulted in a solid, which was washed with THF and ether and dried to give the product as a red crystalline solid (138 mg, 60%). IR (KBr): $\nu_{OH}$ 3594 $cm^{-1}$. Absorption spectrum (DMF): $\lambda_{max}$ ($\varepsilon_M$) 411 (5500), 483 (sh, 2600) nm. $^1$H NMR ($CD_2Cl_2$): $\delta$ −4.95 (s, 1), 2.48 (s,

(16) Panda, R.; Berlinguette, C. P.; Zhang, Y.; Holm, R. H. *J. Am. Chem. Soc.* **2005**, *127*, 11092–11101.
(17) Sun, J.; Tessier, C.; Holm, R. H. *Inorg. Chem.* **2007**, *46*, 2691–2699.
(18) Hikichi, S.; Ogihara, T.; Fujisawa, K.; Kitajima, N.; Akita, M.; Morooka, Y. *Inorg. Chem.* **1997**, *36*, 4539–4547.
(19) MacBeth, C. E.; Hammes, B. S.; Young, V. G., Jr.; Borovik, A. S. *Inorg. Chem.* **2001**, *40*, 4733–4741.
(20) Bénisvy, L.; Halut, S.; Donnadieu, B.; Tuchagues, J.-P.; Chottard, J.-C.; Li, Y. *Inorg. Chem.* **2006**, *45*, 2403–2405.
(21) Bennett, M. A.; Jin, H.; Willis, A. C. *J. Organomet. Chem.* **1993**, *451*, 249–256.
(22) Cámpora, J.; Palma, P.; del Rio, D.; Álvarez, E. *Organometallics* **2004**, *23*, 1652–1655.
(23) Johansson, R.; Wendt, O. F. *Organometallics* **2007**, *26*, 2426–2430.

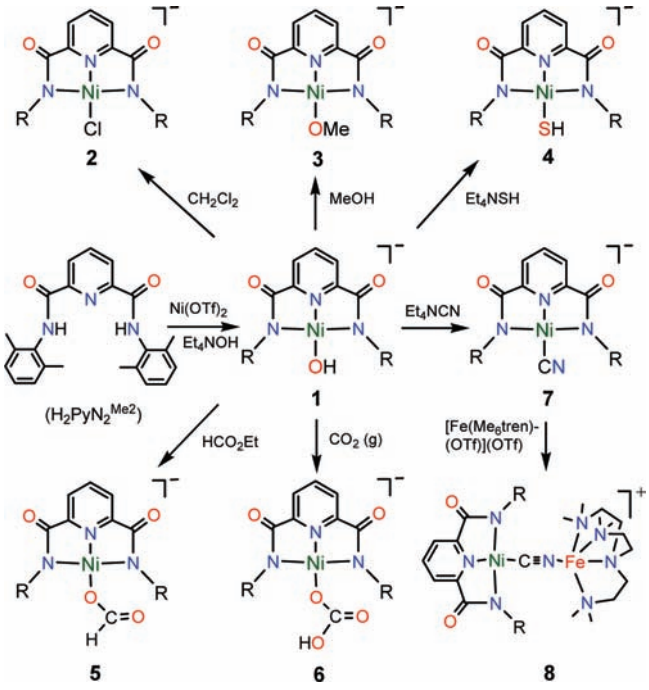


***Figure 2.*** Scheme showing the preparation of pincer complexes $[Ni(pyN_2^{Me2})L]^{1-}$, including hydroxo complex **1** and complexes **2**—**7** derived from it. Binuclear **8** is obtained from **7**.

12), 6.88 (m, 6), 7.51 (d, 2), 7.87 (t, 1). Anal. Calcd for $C_{31}H_{42}N_4NiO_3$: C, 64.49; H, 7.33; N, 9.70. Found: C, 64.36; H, 7.40; N, 9.69.

**$(Et_4N)[Ni(pyN_2^{Me2})Cl]$.** A solution of $(Et_4N)[Ni(pyN_2^{Me2})(OH)]$ (29 mg, 0.050 mmol) in dichloromethane (1 mL) was allowed to stand for 4 d. Ether was diffused into the solution causing deposition of the product as block-like brown-red crystals (24 mg, 81%). $^1$H NMR ($CD_2Cl_2$): $\delta$ 2.42 (s, 12), 6.86 (m, 6), 7.57 (d, 2), 7.97 (t, 1).

**$(Et_4N)[Ni(pyN_2^{Me2})(OMe)]$.** The preceding method with use of methanol (1 mL) afforded a red crystalline product (21 mg, 71%). $^1$H NMR ($CD_2Cl_2$): $\delta$ 2.50 (s, 12), 3.26 (s, 3), 6.89 (m, 6), 7.54 (d, 2), 7.89 (t, 1).

**$(Et_4N)[Ni(pyN_2^{Me2})(SH)]$.** To a solution of $(Et_4N)[Ni(pyN_2^{Me2})(OH)]$ (23 mg, 0.040 mmol) in DMF (1 mL)was added a solution of $Et_4NSH$ (9.8 mg, 0.040 mmol) in an equal volume of DMF. The reaction mixture was stirred for 50 min and filtered. Diffusion of ether into the deep red filtrate gave the product as red crystals (22 mg, 93%). $^1$H NMR (DMF-$d_7$): $\delta$ −3.51 (s, 1), 2.36 (s, 12), 6.81 (m, 6), 7.66 (d, 2), 8.19 (t, 1). Anal. Calcd for $C_{31}H_{42}N_4NiO_2S$: C, 62.74; H, 7.13; N, 9.44. Found: C, 62.64; H, 7.17; N, 9.44.

**$(Et_4N)[Ni(pyN_2^{Me2})(HCO_2)]$.** A solution of $(Et_4N)[Ni(pyN_2^{Me2})(OH)]$ (12 mg, 0.020 mmol) in DMF (0.5 mL) was layered with ethyl formate (4 mL). After 2 d, the product was collected as orange-red crystals (7.0 mg, 58%). IR (KBr): 1615 (s), 1587 (w), 1470 (m), 1437 (vw), 1368 (m), 1300 (m) cm$^{-1}$. $^1$H NMR ($CD_2Cl_2$): $\delta$ 2.49 (s, 12), 6.85 (m, 6), 7.54 (d, 2), 7.94 (t, 1). Anal. Calcd for $C_{32}H_{42}N_4NiO_4$: C, 63.49; H, 6.99; N, 9.26. Found: C, 63.85; H, 7.10; N, 9.11.

**$(Et_4N)[Ni(pyN_2^{Me2})(HCO_3)]$.** A solution of $(Et_4N)[Ni(pyN_2^{Me2})(OH)]$ (23 mg, 0.040 mmol) in DMF (2 mL) was bubbled with carbon dioxide for 15 min. Diffusion of ether into the red solution gave the product as orange-red crystals (21 mg, 85%). IR (KBr): 1618 (vs), 1585 (w), 1470 (m), 1439 (w), 1360 (s), 1310 (w) cm$^{-1}$. Absorption spectrum (DMF): $\lambda_{max}$ ($\varepsilon_M$) 300 (sh, 7800), 381 (5500), 476 (sh, 1500) nm. $^1$H NMR ($CD_3CN$): $\delta$ 2.40 (s, 12), 6.90 (s, 6), 7.63 (s, 2), 8.15 (t, 1). Anal. Calcd for $C_{32}H_{42}N_4NiO_5$: C, 61.85; H, 6.81; N, 9.02. Found: C, 61.44; H, 7.07; N, 8.99.

**$(Et_4N)[Ni(pyN_2^{Me2})(CN)]$.** To a solution of $(Et_4N)[Ni(pyN_2^{Me2})(OH)]$ (23 mg, 0.040 mmol) in DMF (1 mL) was added a solution of $Et_4NCN$ (9.4 mg, 0.060 mmol) in DMF (0.5 mL). The reaction mixture was stirred for 1 h and filtered. Ether diffusion into the filtrate caused separation of the product as orange-red crystals (19 mg, 81%). IR (KBr): $\nu_{CN}$ 2127 cm$^{-1}$. $^1$H NMR ($CD_2Cl_2$): $\delta$ 2.40 (s, 12), 6.90 (m, 6), 7.69 (d, 2), 8.07 (t, 1).

**$[Ni(pyN_2^{Me2})(CN)Fe(Me_6tren)](OTf)$.** To a solution of $(Et_4N)[Ni(pyN_2^{Me2})(CN)]$ (19 mg, 0.032 mmol) in DMF (1 mL) was added a solution of $[Fe(Me_6tren)(OTf)](OTf)$[24] (19 mg, 0.032 mmol) in DMF (1 mL). The reaction mixture was stirred for 40 min and filtered. Diffusion of ether into the filtrate affords the product as thin platelike light red crystals (12 mg, 42%). IR (KBr): $\nu_{CN}$ 2135 cm$^{-1}$.

**$(Et_4N)[Pd(pyN_2^{Me2})(OH)]$.** $H_2pyN_3^{Me2}$ (75 mg, 0.20 mmol) and $[Pd(MeCN)_4](OTf)_2$[25] (114 mg, 0.2 mmol) were stirred in acetonitrile for 90 h. Solvent was reduced to ca. 3 mL and ether (13 mL) added to deposit a yellow-brown solid, which was washed with acetonitrile/THF (2 mL, 1:3 v/v) and dried. The solid was dissolved in DMF/THF (4 mL, 1:3 v/v), and the yellow solution was treated with $Et_4NOH$ (25% in methanol, 118 mg, 0.20 mmol) and stirred for 4 h. The mixture was filtered and ether diffused into the filtrate to afford the product as light yellow-brown crystalline solid, which was washed with THF and dried in vacuo (88 mg, 70%). Absorption spectrum (DMF): $\lambda_{max}$ ($\varepsilon_M$) 335 (8600) nm. $^1$H NMR (DMF-$d_7$): $\delta$ −3.14 (s, 1), 2.35 (s, 12), 6.83 (t, 2), 6.92 (d, 4), 7.74 (d, 2), 8.20 (t, 1).

**$(Et_4N)[Pd(pyN_2^{Me2})(HCO_3)]$.** A solution of $(Et_4N)[Pd(pyN_2^{Me2})(OH)]$ (25 mg, 0.040 mmol) in DMF was bubbled with carbon dioxide for 30 min. Diffusion of ether into the solution resulted in separation of the product as block-like yellow crystals (24 mg, 90%). IR (KBr): 1615 (vs), 1584 (w), 1469 (m), 1445 (s), 1366 (s), 1304 (w) cm$^{-1}$. Absorption spectrum (DMF): $\lambda_{max}$ ($\varepsilon_M$) 276 (sh, 8800), 335 (sh, 5000) nm. $^1$H NMR (DMF-$d_7$): $\delta$ 2.36 (s, 12), 6.78 (t, 2), 6.85 (d, 4), 7.74 (d, 2), 8.28 (t, 1).

**(b) Macrocyclic Ligand and Complexes.** Reactions leading to the ligand and complexes are outlined in Figures 3 and 4.

**Intermediates 9—12.** 3-Nitrobenzaldehyde (7.56 g, 50 mmol) and 3-*N*-methylaminopentane-1,5-diamine (2.93 g, 25 mmol) were reacted in ethanol (150 mL) for 12 h. The solid collected by filtration and a second batch obtained by volume reduction of the filtrate were combined and washed with ethanol to afford light yellow **9** (8.63 g, 90%; $^1$H NMR ($CDCl_3$) $\delta$ 2.41 (s, 3), 2.83 (t, 4), 3.78 (t, 4), 7.51 (t, 2), 8.00 (d, 2), 8.21 (d, 2), 8.32 (s, 2), 8,48 (s, 2)). $NaBH_4$ (3.40 g, 90 mmol) was added to a solution of **9** (8.63 g, 22.5 mmol) in methanol (150 mL) at 50 °C. The solution was cooled to room temperature, solvent was removed, and the orange solid was extracted with dichloromethane/water (200 mL/100 mL). The organic layer was washed with water (2 × 100 mL), dried over $MgSO_4$, and filtered. Removal of solvent gave **10** as a pale yellow oil (7.67 g, 88%; $^1$H NMR ($CDCl_3$) $\delta$ 1.85 (s, br, 2), 2.20 (s, 3), 2.52 (t, 4), 2.70 (t, 4), 3.90 (s. 4), 7.45 (t, 2), 7.64 (d, 2), 8.07 (d, 2), 8.20 (s, 2)). To a solution of **10** (7.67 g, 20 mmol) in acetonitrile (540 mL) and acetic acid (60 mL) was added an aqueous solution of formaldehyde (28 mL, 37%). The mixture was stirred for 1 h and cooled to 0 °C, and $NaBH_4$ (3.74 g, 99 mmol) was slowly added. Stirring was continued for 2 h and for 36 h at room temperature. After filtration, solvent was removed from the filtrate to give a light yellow sticky solid, which was stirred in dichloromethane (200 mL). A solution of 2 M NaOH was added until the pH was ca. 14. The aqueous layer was extracted with dichloromethane (2 × 50 mL), and the combined organic layers were washed with water (100 mL), dried over $MgSO_4$, and filtered. Removal of solvent from the filtrate gave **11** as a light yellow oil (7.07 g, 86%; $^1$H NMR ($CDCl_3$) $\delta$ 2.21 (s, 6), 2.22 (d, 3), 2.53 (m,

(24) Britovsek, G. J. P.; England, J.; White, A. J. P. *Inorg. Chem.* **2005**, *44*, 8125–8134.
(25) Wendt, O. F.; Kaiser, N.-F. K.; Elding, L. I. *J. Chem. Soc., Dalton Trans.* **1997**, 4733–4737.

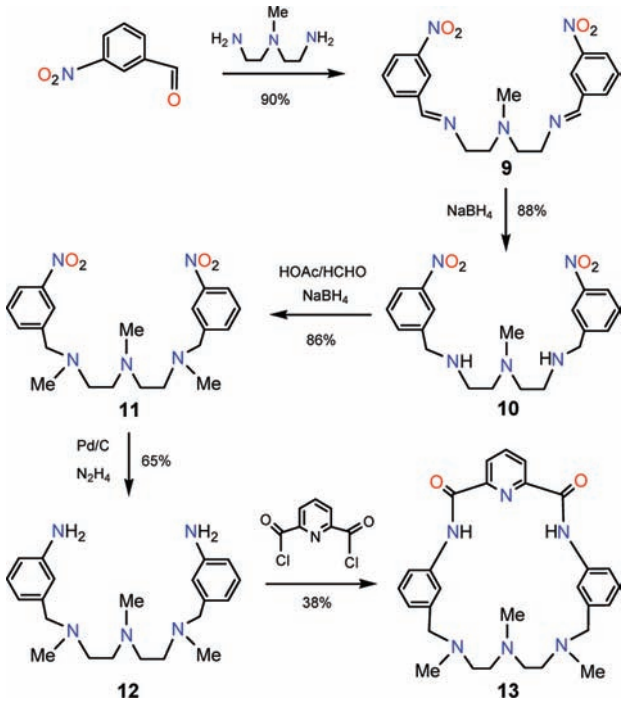


***Figure 3.*** Scheme for the synthesis of the binucleating pincer macrocycle ⊂-$H_2$py$N_2$dien$^{Me3}$ (**13**).

8), 3.59 (s, 4), 7.45 (t, 2), 7.64 (d, 2), 8.08 (d, 2), 8.19 (s, 2)). To a mixture of **11** (2.49 g, 6.0 mmol) and Pd/C (160 mg) in anhydrous ethanol was added a solution of $N_2H_4 \cdot H_2O$ (20 mL). The mixture was stirred for 30 min and for 12 h at 60 °C and filtered. Volume reduction of the filtrate gave a light orange oil. The crude product was purified in the air on a silica column eluted with dichloromethane/methanol/$NH_4OH$ to give **12** as a light yellow oil (1.38 g, 65%; $^1$H NMR ($CDCl_3$) $\delta$ 2.18 (s, 3), 2.19 (s, 6), 2.49 (m, 8), 3.39 (s, 2), 3.43 (s, 2), 3.68 (s, br, 4), 6.55 (d, 2), 6.66 (m, 4), 7.06 (t, 2)).

**⊂-$H_2$py$N_2$dien$^{Me3}$.** To a solution of $Et_3N$ (13 mL) in THF (350 mL) was added simultaneously solutions of **12** (1.38 g, 3.90 mmol) and pyridine-2,6-dicarbonyl chloride (0.79 g, 3.90 mmol), each in THF (50 mL), by syringe pump over 24 h. The reaction mixture was stirred for 3 h and filtered, and the filtrate was evaporated to leave a yellow-orange solid. This residue was stirred with methanol (120 mL, 1 h), and the solution was filtered. The yellow filtrate was reduced to ca. 6 mL and heated to dissolve any solid. Cooling the solution caused separation of colorless crystals. The steps of filtrate volume reduction and cooling were repeated several more times to obtain additional amounts of white crystals. The crops were combined and dried to give the product as a white solid (0.72 g, 38%). $^1$H NMR (DMSO-$d_6$): $\delta$ 2.13 (s, 6), 2.25 (s, 3), 2.53 (t, 4), 2.60 (t, 4), 3.51 (s, 4), 7.01 (d, 2), 7.35 (t, 2), 7.66 (s, 2), 8.30 (t, 1), 8.39 (m, 4), 11.22 (s, 2). Anal. Calcd for $C_{28}H_{34}N_6O_2$: C, 69.11; H, 7.04; N, 17.27. Found: C, 68.01; H, 7.03; N, 17.01.

**($Et_4$N)[Ni(OH)(⊂-py$N_2$dien$^{Me3}$)].** The macrocycle (73 mg, 0.15 mmol) and $Ni(OTf)_2$ (53 mg, 0.15 mmol) were mixed and stirred in DMF (2 mL) for 1 h to give a light yellow suspension. $Et_4NOH$ (25% in methanol, 118 mg, 0.20 mmol) was added, and the mixture was stirred for 2 h forming a red suspension. A second portion of $Et_4NOH$ (147 mg, 0.25 mmol) was added, and the mixture was stirred to 10 h to give a deep red solution with some sticky precipitate. The latter was removed by filtration through Celite. Addition of ether (25 mL) to the filtrate and storage at −20 °C for 2 d yielded the product as red crystals (53 mg, 51%). IR (KBr): $\nu_{OH}$ 3606 cm$^{-1}$. Absorption spectrum (DMF): $\lambda_{max}$ ($\varepsilon_M$) 411 (5400), 483 (sh, 1900) nm. $^1$H NMR (DMF-$d_7$): $\delta$ −4.40 (s, 1), 2.01 (s, 3), 2.20 (m, 4), 2.28 (m, 10), 3.35 (s, 4), 6.80 (d, 2), 7.05 (t, 2), 7.20 (s, 2), 7.28 (d, 2), 7.54 (d, 2), 8.06 (t, 1).

**($Et_4$N)[Ni($HCO_3$)(⊂-py$N_2$dien$^{Me3}$)].** A solution of ($Et_4$N)[Ni(OH)(⊂-py$N_2$dien$^{Me3}$)] (21 mg, 0.030 mmol) in DMF (1.5 mL) was bubbled with carbon dioxide for 15 min. Diffusion of ether in the red solution caused separation of the product as orange-red crystals (17 mg, 77%). IR (KBr): 1656 (s), 1619 (vs), 1580 (m), 1481 (w), 1456 (m), 1369 (m), 1328 (s) cm$^{-1}$. Absorption spectrum (DMF): $\lambda_{max}$ ($\varepsilon_M$) 381 (5500), 476 (sh, 880) nm. $^1$H NMR ($CD_3CN$): $\delta$ 1.88 (s, 3), 2.21 (br, s, 4), 2.32 (s, 6), 2.42 (br, s, 4), 3.43 (br, s, 4), 6.78 (d, 2), 6.90 (d, 2), 7.02 (s, 2), 7.09 (t, 2), 7.75 (d, 2), 8.01 (t, 1).

**($Et_4$N)[Ni(CN)(⊂-py$N_2$dien$^{Me3}$)].** To a solution of ($Et_4$N)[Ni(OH)(⊂-py$N_2$dien$^{Me3}$)] (34.5 mg, 0.050 mmol) in DMF (2 mL) was added a solution of $Et_4NCN$ (7.8 mg, 0.050 mmol) in DMF (1 mL). The reaction mixture was stirred for 1 h and filtered. Addition of ether (15 mL) to the red filtrate deposited the product as an orange crystalline solid (26 mg, 75%). IR (KBr): $\nu_{CN}$ 2129 cm$^{-1}$.

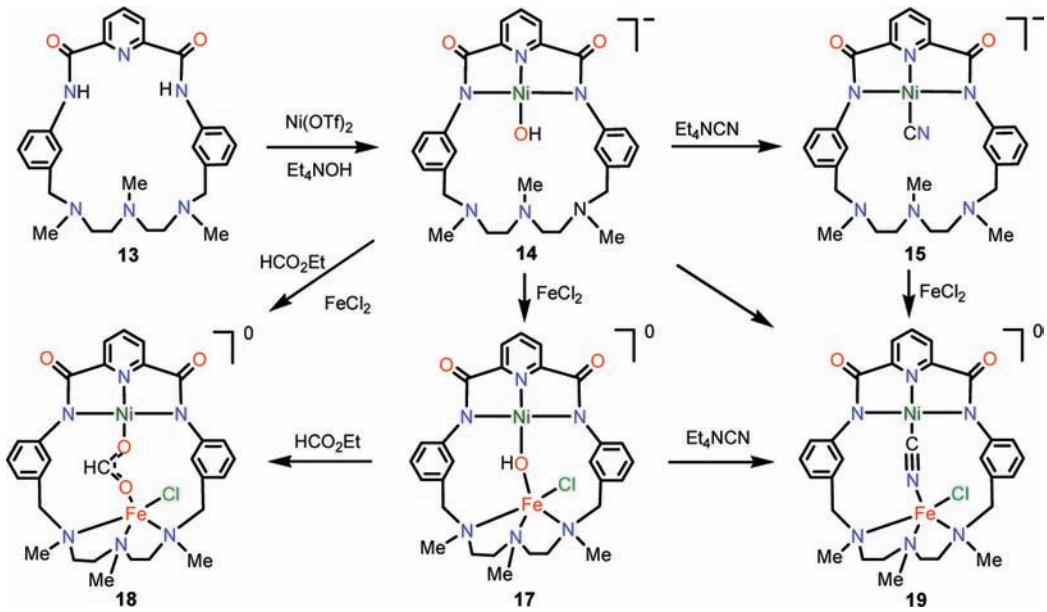


***Figure 4.*** Preparation of macrocyclic complexes [Ni(L)(⊂-py$N_2$dien$^{Me3}$)]$^{1-}$ with L = $OH^-$ (**14**) and $CN^-$ (**15**) and bridged complexes [Ni(L)FeCl(⊂-py$N_2$dien$^{Me3}$)] with L = $OH^-$ (**17**), $HCO_2^-$ (**18**), and $CN^-$ (**19**).

$^1$H NMR ($CD_2Cl_2$): $\delta$ 2.24 (s, 3), 2.32 (s, 6), 2.49 (m, 4), 2.60 (m, 4), 3.51 (s, 4), 6.86 (d, 2), 7.03 (d, 2), 7.08 (t, 2), 7.41 (s, 2), 7.66 (d, 2), 8.00 (t, 1).

**[Ni(OH)FeCl(⊂-pyN$_2$dien$^{Me3}$)].** To a solution of ($Et_4N$)[Ni(OH)(⊂-pyN$_3$dien$^{Me3}$)] (28 mg, 0.040 mmol) in DMF (2 mL) was added a solution of $FeCl_2$ (5.1 mg, 0.040 mol) in DMF (1 mL). The reaction mixture was stirred for 1 h, filtered through Celite, and ether was slowly diffused into the deep red filtrate over 3 d. The crystalline solid was washed with acetonitrile (5 mL) and dried to afford the product as red crystals (10 mg, 38%). IR (KBr): $\nu_{OH}$ 3597 cm$^{-1}$. Anal. Calcd for $C_{28}H_{33}ClFeN_6NiO_3$: C, 51.61; H, 5.11; N, 12.90; Fe, 8.57; Ni, 9.01. Found: C, 51.44; H, 5.39; Fe, 8.47; N, 12.79; Ni, 8.88.

**[Ni(HCO$_2$)FeCl(⊂-pyN$_2$dien$^{Me3}$)].** To a solution of ($Et_4N$)[Ni(OH)(⊂-pyN$_2$dien$^{Me3}$)] (28 mg, 0.040 mmol) in DMF (1 mL) was added a solution of $FeCl_2$ (5.1 mg, 0.040 mmol) in DMF (1 mL). The reaction mixture was stirred for 1 h and filtered through Celite. The deep red filtrate was layered with ethyl formate (4 mL) for 4 d, filtered, and ether diffused into the filtrate to deposit the product as a red crystalline solid (8.0 mg, 30%). IR (KBr): 1631 (vs), 1599 (vs), 1485 (w), 1462 (m), 1441 (w), 1366 (s), 1311 (w) cm$^{-1}$.

**[Ni(CN)FeCl(⊂-pyN$_2$dien$^{Me3}$)].** To a solution of ($Et_4N$)[Ni(CN)(⊂-pyN$_2$dien$^{Me3}$)] (26 mg, 0.037 mmol) in DMF (1 mL) was added a solution of $FeCl_2$ (4.7 mg, 0.050 mmol) in DMF (0.5 mL). The reaction mixture was stirred for 1 h, filtered, and ether was added to the orange-red filtrate. The deposited solid was washed with acetonitrile (3 mL), stirred with methanol (1 mL) to form a suspension, which was filtered. The solid was dissolved in $Me_2SO$/DMF/methanol (1:1:1 v/v/v, 1.5 mL) and ether added by diffusion to give the product as orange crystals (8.0 mg, 33%). IR (KBr): $\nu_{CN}$ 2154 cm$^{-1}$.

**Attempted Reactions with Carbon Monoxide.** No reaction was detected when CO was bubbled through DMF solutions of $Ni^{II}$ hydroxo complexes **1** and **14** for 15−20 min. The same treatment of **17** led to an off-white ill-defined solid after ether diffusion into the reaction mixture, and with $Pd^{II}$ hydroxo complex **20** a black precipitate formed within ca. 2 min, and no further reaction occurred after 20 min. Under similar conditions, all complexes but **17** readily formed soluble bicarbonate complexes with $CO_2$.

**X-ray Structure Determinations.** The structures of the 15 compounds in Tables S1−S3 (Supporting Information) were determined; for brevity they are referred to by their anion or cation number. Diffraction-quality crystals were obtained from the following solvents: DMF/ether (**1**, **4**, **6**−**8**, **14**, **17**, **20**, **21**), dichloromethane/ether (**2**), methanol/ether (**3**, **13**), DMF/ethyl formate (**5**, **18**), and $Me_2SO$/DMF/methanol/ether (**19**). Diffraction data were collected on a Bruker CCD area detector diffractometer equipped with an Oxford 700 low temperature apparatus. Single crystals were coated with Paratone-N oil and mounted on a Nylon loop. Structures were solved by direct methods using the SHELX program package.[26] Hydrogen atoms were not added to the cations or solvate molecules in **1**−**3**, **6**, **7**, **14**, **18**, and **20** owing to disordered carbon atoms but are included in the compound formulas. In **13**, hydrogen atoms of two HCl molecules were not located from Fourier maps but are included for charge balance. The hydrogen atoms of the −OH groups in **1**, **14**, **17**, the −SH group in **4**, and the $-HCO_3$ group in **6** and **21** were located from difference Fourier maps and refined isotropically. Crystal data and refinement details are given in Tables S1−S3 (Supporting Information).[27]

**Other Physical Measurements.** Absorption spectra were determined with a Cary 50 Bio spectrophotometer. $^1$H NMR spectra were recorded on a Varian AM-400 instrument. Infrared spectra were obtained with a Nicolet 5PCFT-IR spectrometer.

## Results and Discussion

Because the $CO_2$ intermediate (b) and cyanide-inhibited C-clusters (Figure 1, (c, d)) involve binding to nickel, we first focused attention on reactions at $Ni^{II}$ in an NNN pincer ligand environment. Reaction of deprotonated *N*,*N*′-bis(phenyl)-2,6-pyridinedicarboxamide and $NiCl_2$(dme) in a 2:1 molar ratio affords octahedral $[Ni(pyN_2)_2]^{2-}$.[28] When the reaction is conducted with a 1:1 ratio, we find the same complex formed (in reduced yield) owing to the favorable *d*-electron stabilization of octahedral $d^8$. However, with 1:1 deprotonated *N*,*N*′-bis(2,6-diisopropylphenyl)-2,6-pyridinedicarboxamide and $Ni^{II}$, the planar monopincer complexes [Ni(pyN$_2^{iPr2}$)L] (L = $OH_2$, $PMe_3$) result.[29] Lesser steric hindrance that destabilizes a bis-pincer complex occurs with 2,6-dimethylphenyl *N*-substituents, as shown by formation of the $[Ni(pyN_2^{Me2})L]^{1-}$ series of complexes **1**−**7** (Figure 2).

**Mononuclear $Ni^{II}$ Binding and Structures.** The key species in the foregoing series is hydroxo complex **1**, readily formed by deprotonation of the pincer ligand with $Et_4NOH$ in the presence of $Ni(OTf)_2$ in THF and obtained in 60% yield. Compared to the double bridge $Ni^{II}(OH)_2Ni^{II}$ [30,31] and the supported bridge Ni−(OH)−Ni,[32,33] the terminal $Ni^{II}$−OH group is uncommon[23,34−37] and is usually stabilized by hydrogen bonding or, as is the case here, by steric protection. The upfield −OH resonance ($\delta$ −4.95), similar in position to other Ni−OH groups,[30,38] is indicative of nucleophilic reactivity, as displayed in reaction with dichloromethane (**2**, 81%) and reactions 1 with ethyl formate (**5**, 58%) and $CO_2$ (**6**, 85%)). The complex deprotonates methanol (**3**, 71%) and undergoes substitution by L = $HS^-$ (**4**, 93%) or $CN^-$ (**7**, 81%) in reaction 2. Products were isolated as $Et_4N^+$ salts in the indicated yields. It was also demonstrated that **7** reacts with $[Fe(Me_6tren)(OTf)]^{1+}$ to form binuclear complex **8**, obtained as the triflate salt (42%).

$$[Ni(pyN^{Me2})_2(OH)]^{1-} + HCO_2Et/CO_2 \rightarrow [Ni(pyN^{Me2})_2(HCO_2)/(HCO_3)]^{1-} + EtOH/- - \quad (1)$$

$$[Ni(pyN^{Me2})_2(OH)]^{1-} + L^- \rightarrow [Ni(pyN^{Me2})_2L]^{1-} + OH^- \quad (2)$$

The complexes **1**−**7** are planar; structures of hydroxo, formate, bicarbonate, and cyanide complexes are set out in Figure 5. Because dimensions of the $NiN_3$ portions of the coordination units are practically invariant, only the values for

(26) Sheldrick, G. M. *Acta Crystallogr.* **2009**, *A64*, 112–122.
(27) See the paragraph at the end of this article for Supporting Information available.
(28) Patra, A. K.; Mukherjee, R. *Inorg. Chem.* **1999**, *38*, 1388–1393.
(29) Wasilke, J.-C.; Wu, G.; Bu, X.; Kehr, G.; Erker, G. *Organometallics* **2005**, *24*, 4289–4297.
(30) Carmona, E.; Marín, J. M.; Palma, P.; Paneque, M.; Poveda, M. L. *Inorg. Chem.* **1989**, *28*, 1895–1900.
(31) Kitajima, N.; Hikuchi, S.; Tanaka, M.; Moro-oka, Y. *J. Am. Chem. Soc.* **1993**, *115*, 5496–5508.
(32) Barrios, A. M.; Lippard, S. J. *J. Am. Chem. Soc.* **2000**, *122*, 9172–9177.
(33) Kersting, B. *Angew. Chem., Int. Ed.* **2001**, *40*, 3988–3990.
(34) Orlandini, A.; Sacconi, L. *Inorg. Chem.* **1976**, *15*, 78–85.
(35) Meyer, F.; Kaifer, E.; Kircher, P.; Heinze, K.; Pritzkow, H. *Chem.−Eur. J.* **1999**, *5*, 1617–1630.
(36) Cámpora, J.; Matas, I.; Palma, P.; Graiff, C.; Tiripicchio, A. *Organometallics* **2005**, *24*, 2827–2830.
(37) Kieber-Emmons, M. T.; Schenker, R.; Yap, G. P. A.; Brunold, T. C.; Riordan, C. G. *Angew. Chem., Int. Ed.* **2004**, *43*, 6716–6718.
(38) López, G.; Garcia, G.; Sánchez, G.; Garcia, J.; Vicente, C. *J. Chem. Soc., Chem. Commun.* **1989**, 1045–1046.

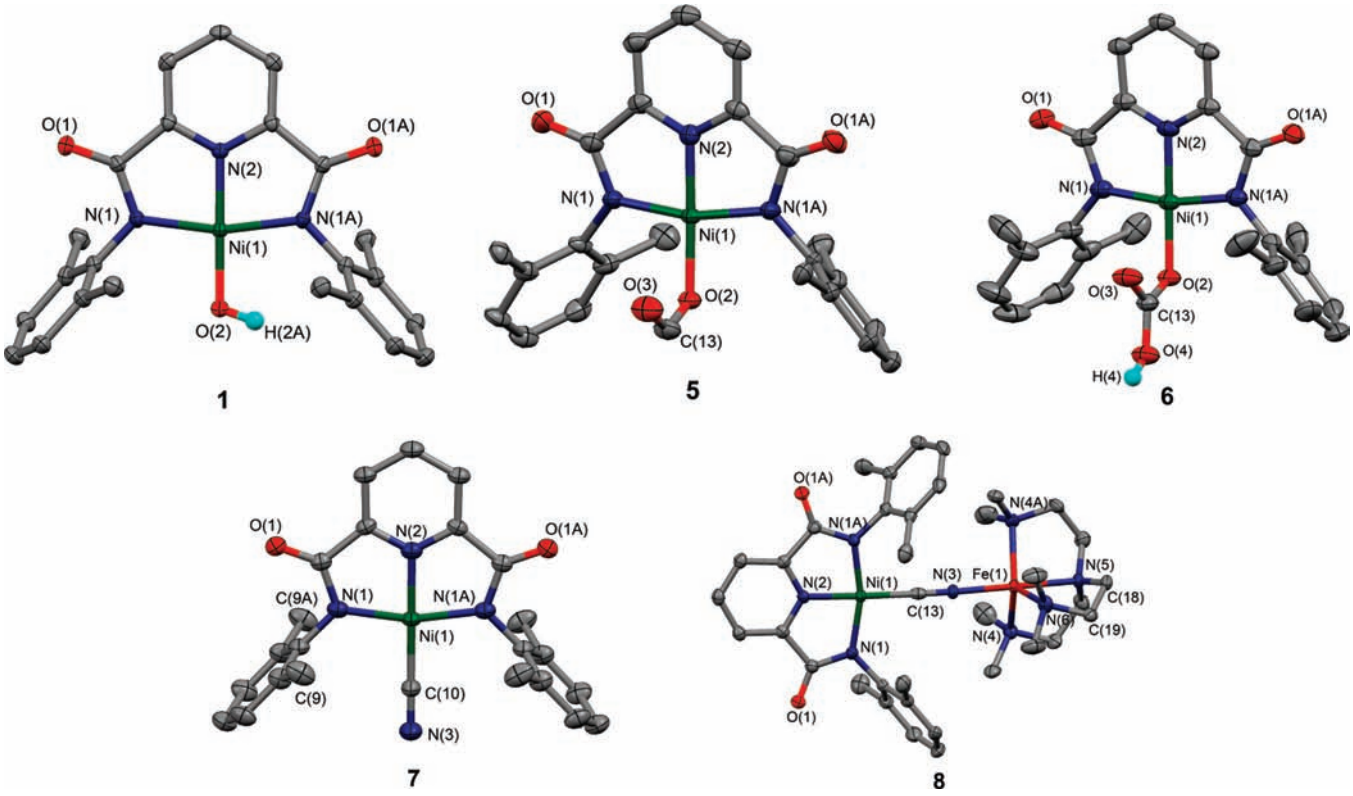


***Figure 5.*** Structures of five pincer complexes $[Ni(pyN_2^{Me2})L]^{1-}$ with L = $OH^-$ (**1**), $HCO_2^-$ (**5**), $HCO_3^-$ (**6**), $CN^-$ (**7**), and (CN)Fe(tren)$^{1+}$ (**8**). Atom numbering schemes and 50% probability ellipsoids are shown. Selected bond distances (Å) and angles (deg). **1**: Ni−N1, 1.911(2); Ni−N2, 1.826(3); Ni−O2, 1.825(3); N1−Ni−N2, 82.73(7); N1−Ni−O2, 97.29(6); N1−Ni−N1A, 165.4(1); N2−Ni−O2, 176.9(1). **5**: Ni−O2, 1.857(5); C13−O2, 1.27(1); C13−O3, 1.21(1); Ni−O2−C13, 114.2(5); O2−C13−O3, 127.4(8). **6**: Ni−O2, 1.817(4); C13−O2, 1.253(7); C13−O3, 1.286(7); C13−O4, 1.293(6); Ni−O2−C13, 113.4(3); O2−C13−O3, 121.5(5); O2−C13−O4, 118.5(5); O3−C13−O4, 120.0(5). **7**: Ni−C10, 1.849(7); C10−N3, 1.15(1); Ni−C10−N3, 180.0. **8**: Ni−C13, 1.853(7); C13−N3, 1.129(8); Fe−N3, 2.085(5); av Fe−N(4−6), 2.146[8]; N3−Fe−N5, 179.9(2). Atoms N(1) and N(1A) and O(1) and O(1A) are related by a mirror plane. Disorder of the carbon atoms of a phenyl ring (**5**) and of methylene carbon atoms (**8**) over two equally populated positions is omitted; one position in shown for each molecule.

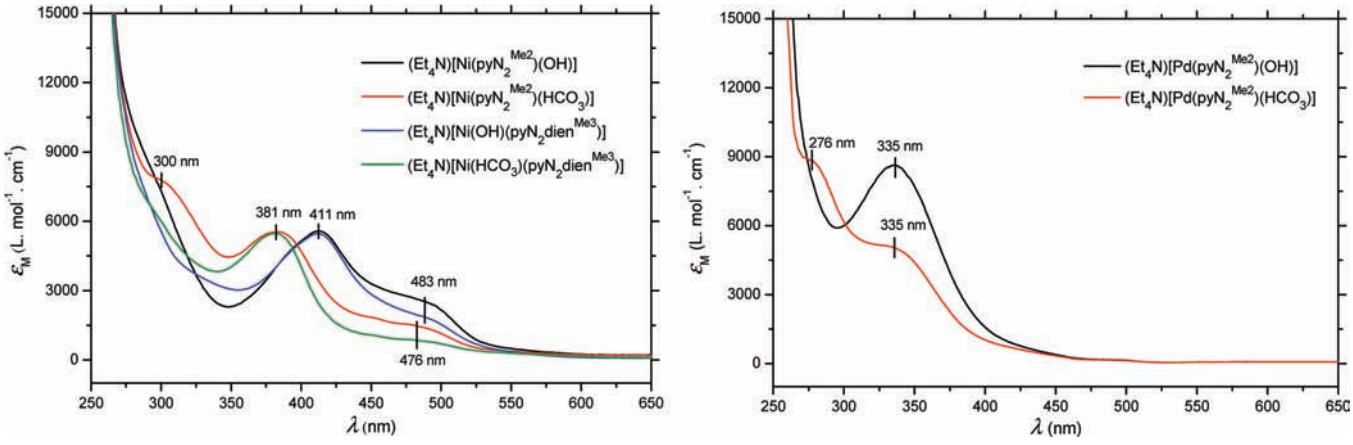


***Figure 6.*** Absorption spectra for the conversion of $Ni^{II}$ and $Pd^{II}$ hydroxo to bicarbonate complexes in DMF upon reaction with $CO_2$. Left: **1** → **5** and **14** → **16**. Right: **20** → **21**.

**1** are given. Cyanide, an inhibitor of CODH which binds at nickel (Figure 1), forms a linear Ni−C≡N unit in **7**. Reaction with ethyl formate gives **5** with bent formate binding (Ni−O2−C13 = 114.2(5)°) and a dihedral angle of 90° between the formate and $NiN_3$ planes. Bicarbonate complex **6** was prepared by passing $CO_2$ through a DMF solution of **1** and can also be obtained by exposure of **1** to the air in an immediate reaction. As observed in Figure 6, UV−vis spectral changes associated with the reaction are very clear, resulting in a shift of the most intense band from 411 to 381 nm. Bicarbonate binding is very similar to formate, coordinating in the $\eta^1$ mode with Ni−O2−C13 = 113.4(3)° and a $CO_3/NiN_3$ dihedral angle of 90°. These are the initial examples of the reaction of a terminal $Ni^{II}$−OH group with a formate ester or $CO_2$ itself, leading to the first structure

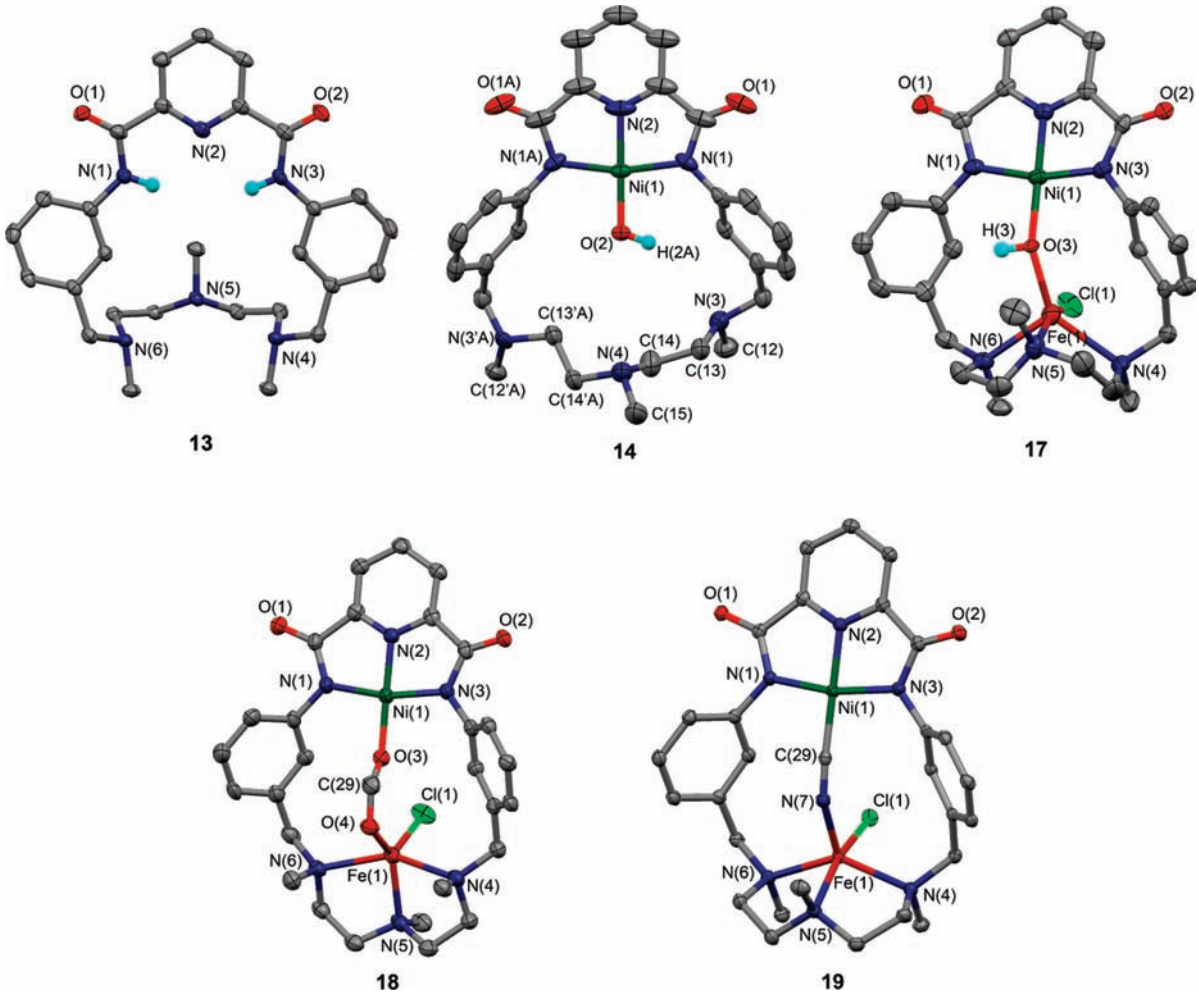


***Figure 7.*** Structures of free macrocycle ⊂-$H_2pyN_2dien^{Me3}$ (**13**), [Ni(OH)(⊂-$pyN_2dien^{Me3}$)]$^{1-}$ (**14**), and [Ni(L)FeCl(⊂-$pyN_2dien^{Me3}$)] with L = $OH^-$ (**17**), $HCO_2^-$ (**18**), $CN^-$ (**19**). Atom numbering schemes and 50% probability ellipsoids are shown. Selected bond distances (Å) and angles (deg). **14**: Ni−N1, 1.927(4); Ni−N2, 1.821(6); Ni−O2, 1.802(4); N1−Ni−N2, 82.7(1); N1−Ni−O2, 97.3(1). **17**: Ni−O3, 1.927(4); Fe−O3, 2.059(3); Fe−Cl, 2.334(2); Ni−O3−Fe, 140.0(2); Ni···Fe, 3.747(2). **18**: Ni−O3, 1.842(3); Fe−O4, 2.032(3); Fe−Cl, 2.252(2); C29−O3, 1.216(6); C29−O4, 1.236(5); Ni−O3−C29, 135.9(3); O3−C29−O4, 125.2(4); Fe−O4−C29, 120.2(3); Ni···Fe, 4.792(1). **19**: Ni−C29, 1.827(3); C29−N7, 1.145(4); Fe−N7, 2.022(2); Ni−C29−N7, 170.3(3); Fe−N7−C29, 141.8(2); Ni···Fe, 4.631(1). Complex **18** occurs as two independent molecules of very similar structure; the data refer to one structure. Disorder in the positions of certain nitrogen and carbon atoms in a 1:1 population in **14** is omitted; only one position is shown.

proofs of the binding modes $Ni^{II}$−($\eta^1$-OCHO) and $Ni^{II}$−($\eta^1$-OC(O)OH) (vide infra). In comparison to these reactions, **1** does not react with CO.

**Macrocyclic Mononuclear $Ni^{II}$ and Binuclear $Ni^{II}Fe^{II}$ Systems.** Having examined the reactivity of the NNN pincer $Ni^{II}$ site in mononuclear complexes, a binuclear system containing this site and a binding site for $Fe^{II}$ was sought. We utilized the binucleating macrocycle concept[39,40] with a ligand design related to NCN pincer-crown ethers[41,42] and binding sites differentiated for selective metal incorporation. The target macrocycle ⊂-$H_2pyN_2dien^{Me3}$ (**13**) was synthesized via intermediates **9**−**12** by the reaction sequence in Figure 3, which results in an overall 17% yield from 3-nitrobenzaldehyde. Macrocycle formation was verified by the X-ray structure in Figure 7. The molecule is approximately planar except for the dien-type fragment whose $N_2C_4$ least-squares plane forms a dihedral angle of 82.3° with the least-squares plane of the remainder of the molecule (atom deviations of ≤0.20 Å).

Preparations of mononuclear and binuclear macrocyclic complexes are summarized in Figure 4; structures are reported in Figure 7. Using the same procedure as for **1**, $Ni^{II}$ was taken up in the pincer site to yield hydroxo complex **14** (51%), which was readily converted to cyanide complex **15** by ligand substitution. Binding of $Ni^{II}$ in the macrocycle results in a conformational change in the dien portion and reorientation of the phenyl rings from a dihedral angle of 77.6° with the $NiN_3$ plane in **1** to 60.4° in **14**. Both complexes have mirror symmetry, and metric features of their $NiN_3O$ coordination units are insignificantly different. Bicarbonate complex **16** was prepared from **14** and $CO_2$. An X-ray structure was not determined, but the spectral comparison with **5** (Figure 6) demonstrates formation of the complex.

Three $Ni^{II}Fe^{II}$ complexes, with hydroxo (**17**), formate (**18**), and cyanide bridges (**19**), were prepared. Complexes **17** and

(39) Gavrilova, A. L.; Bosnich, B. *Chem. Rev.* **2004**, *104*, 349–383.
(40) Vigato, P. A.; Tamburini, S.; Bertolo, L. *Coord. Chem. Rev.* **2007**, *251*, 1311–1492.
(41) Mahoney, J. M.; Nawaratna, G. U.; Beatty, A. M.; Duggan, P. J.; Smith, B. D. *Inorg. Chem.* **2004**, *43*, 5902–5907.
(42) Mahoney, J. M.; Stucker, K. A.; Jiang, H.; Carmichael, I.; Brinkmann, N. R.; Beatty, A. M.; Noll, B. C.; Smith, B. D. *J. Am. Chem. Soc.* **2005**, *127*, 2922–2928.

***Table 1.*** Bridge Dimensions (Å, deg) in Macrocyclic Complexes

| | 17 | 18 | 19 |
|---|---|---|---|
| Ni−O | 1.927(4) | 1.842(3) | |
| Fe−O | 2.059(3) | 2.032(3) | |
| Ni−C | | | 1.827(3) |
| Fe−N | | | 2.022(2) |
| Ni−O−Fe | 140.0(2) | | |
| Ni−O−C | | 135.9(3) | |
| Ni−C−N | | | 170.3(3) |
| Fe−O−C | | 120.2(3) | |
| Fe−N−C | | | 141.8(2) |
| O−C−O | | 125.2(4) | |
| Ni···Fe | 3.747(2) | 4.792(1) | 4.631(1) |

**19** were obtained by insertion of $Fe^{II}$ in reactions 3 with **14** (L = $OH^-$, 38%) and **15** (L = $CN^-$, 75%), whereas **18** was prepared from **17** generated in situ and ethyl formate in reaction 4. In these species, $Ni^{II}$ is planar while the $Fe^{II}N_3OCl$ units are intermediate between trigonal pyramidal and square pyramidal ($\tau$ = 0.51 (**17**), 0.43 (**19**)) or approach trigonal bipyramidal ($\tau$ = 0.17, 0.19 (**18**)). The shape parameter $\tau$ = 0 for square pyramidal and 1 for trigonal bipyramidal structures.[43] Ring conformations in the dien region are similar and the $NiN_3$/phenyl dihedral angles (53.5−56.4°) indicate that inclusion of the bridge units has a minor effect on phenyl group orientations in the three complexes. Attempts to prepare complexes with hydroxycarbonyl as bridges were unsuccessful. In particular, **14**, as **1**, is unreactive toward CO and **17** did not yield a tractable product.

$$[Ni(L)(\subset\text{-}pyN_2dien^{Me3})]^{1-} + FeCl_2 \rightarrow [Ni(L)FeCl(\subset\text{-}pyN_2dien^{Me3})] + Cl^- \quad (3)$$

$$[Ni(OH)FeCl(\subset\text{-}pyN_2dien^{Me3})] + HCO_2Et \rightarrow [Ni(HCO_2)FeCl(\subset\text{-}pyN_2dien^{Me3})] + EtOH \quad (4)$$

There are no prior reports of $Ni^{II}$−L−$Fe^{II}$ bridges with L = $OH^-$ and $HCO_2^-$ and only one other case of a single intramolecular $Ni^{II}$−CN−$Fe^{II}$ bridge.[44] The most closely related bridges with these three linking groups are of the unsupported $Cu^{II}$−L−$Fe^{III}$ type[45−48] and require one trivalent metal center for stability. Complexes **17**−**19** provide the first insights into structure modes of the three bridge groups between these elements. The bridges are supported but the macrocycle is sufficiently flexible so as to sustain bond sequences of different lengths, varying from 3.7 to 4.8 Å. Metric data for bridge units are summarized in Table 1. The hydroxo bridge in **17** features an angle of 140° and bond lengths that separate the metal centers by 3.75 Å. Relative to **14,** the Ni−O interaction has increased by ca. 0.12 Å upon bridge formation. In **18**, formate functions as an $\mu_2$:$\eta^2$ bridge with the metal centers in a *syn* orientation, M−O−C bond angles of 136° (M = Ni) and 120° (M = Fe), and a Ni···Fe distance of 4.79 Å. In **19**, the Ni−CN and C≡N bonds are not significantly altered by bridge formation compared to **7**. The complete Ni−C≡N−Fe bridge unit in **8** is linear, whereas in **19** the Ni−C≡N portion is linear but the Fe−N≡C sequence is bent (142°) to a larger extent than in $[Ni(pdtc)CNFe(Me_6tren)]^{1+}$ (166°),[44] the only other molecular example of a single $Ni^{II}$−CN−$Fe^{II}$ bridge. The bent configuration is probably due to macrocycle constraints which with a cyanide bridge impose a 4.63 Å Ni···Fe separation.

**$Ni^{II}$ and $Pd^{II}$ Reactivity with CO and $CO_2$.** Prior reactions of $Ni^{II}$ with $CO_2$ have involved only binuclear hydroxo-bridged complexes, which lead to binuclear products containing $\mu_2$:$\eta^3$-$CO_3$ bridges with one or two chelate rings.[30,31,49] In another case, reaction in methanol affords a $\mu_2$:$\eta^2$ methylcarbonate bridge.[33] These result underscore the unique $Ni^{II}$ $\eta^1$-bicarbonate binding mode in **6**, whose ligand structure prevents bridge formation.

Carbonylation reactions of pincer complexes have recently been summarized.[50] We briefly note several observations pertinent to this work with PCP pincer species. Reaction 5 (M = $Pd^{II}$) affords the $\eta^1$ C-bound hydroxycarbonyl complex; with $CO_2$ the product is the $\eta^1$-bicarbonate complex.[23] Reaction 6 (M = $Ni^{II}$, $Pd^{II}$) with a less hindered ligand forms a binuclear $\eta^2$(C,O):$\mu_2$-$CO_2$ product which with additional CO can be cleaved to the mononuclear $Pd^{II}$ hydroxycarbonyl.[22] These results suggested examination of reactions with the $Pd^{II}$ analogue of the $Ni^{II}$−hydroxo complex **1**.

$$[M(OH)(C_6H_3\text{-}2,6\text{-}(CH_2PBu^t_2)_2)] + CO \rightarrow [M(CO_2H)(C_6H_3\text{-}2,6\text{-}(CH_2PBu^t_2)_2)] \quad (5)$$

$$2[M(OH)(C_6H_3\text{-}2,6\text{-}(CH_2PPr^i_2)_2)] + CO \rightarrow \{[M(C_6H_3\text{-}2,6\text{-}(CH_2PPr^i_2)_2)]_2(CO_2)\} + H_2O \quad (6)$$

Reaction of $[Pd(MeCN)_4]^{2+}$ and $H_2pyN_2^{Me2}$ followed by addition of $Et_4NOH$ gave $(Et_4N)$[**20**] (70%). The complex is isostructural with **1**, having Pd−N1 = 2.023(4) Å, Pd−N2 = 1.906(7) Å, and Pd−O = 1.959(6) Å. Reaction with $CO_2$ affords $(Et_4N)$[**21**] (90%) with $\eta^1$-bicarbonate ligation and Pd−O = 2.041(3) Å.[27] Spectral changes parallel those with $Ni^{II}$ but at higher energies (Figure 6). However, exposure to CO resulted in the formation of an insoluble black precipitate; no tractable product was obtained. It is now apparent that the NNN pincer environment, unlike PCP ligands, with $Ni^{II}$−OH or $Pd^{II}$−OH functional groups does not support either CO binding or formation of a hydroxycarbonyl complex.[51]

## Summary

With use of a binucleating macrocycle whose NNN pincer and triamine portions provide selective metal binding sites, the first examples of $Ni^{II}$−L−$Fe^{II}$-bridged molecules have been synthesized and structural modes of three bridging groups ($\mu_2$−$OH^-$, $\mu_2$:$\eta^2$-$HCO_2^-$ and −$CN^-$) established. Results include necessary supporting information on reactivity and structure at the $Ni^{II}$ site in mononuclear NNN pincer complexes. This investigation is motivated by the biomimetic Ni−CODH C-cluster problem whose difficulties have been noted at the outset. The $Ni^{II}Fe^{II}$ molecules are not site analogues because of substantial structural departures from the native site (Figure 1), but their accessibility and demonstrated bridging capability offer

(43) Addison, A. W.; Nageswara Rao, T.; Reedijk, J.; van Rijn, J.; Verschoor, G. C. *J. Chem. Soc., Dalton Trans.* **1984**, 1349–1356.
(44) Huang, D.; Deng, L.; Sun, J.; Holm, R. H. *Inorg. Chem.* **2009**, *48*, 6159–6166.
(45) Scott, M. J.; Zhang, H. H.; Lee, S. C.; Hedman, B.; Hodgson, K. O.; Holm, R. H. *J. Am. Chem. Soc.* **1995**, *117*, 568–569.
(46) Scott, M. J.; Goddard, C. A.; Holm, R. H. *Inorg. Chem.* **1996**, *35*, 2558–2567.
(47) Scott, M. J.; Holm, R. H. *J. Am. Chem. Soc.* **1994**, *116*, 11357–11367.
(48) Lim, B. S.; Holm, R. H. *Inorg. Chem.* **1998**, *37*, 4898–4908.
(49) Lozano, A. A.; Sáez, M.; Pérez, J.; García, L.; Lezama, L.; Rojo, T.; López, G.; García, G.; Santana, M. D. *Dalton Trans.* **2006**, 3906–3911.
(50) Morales-Morales, D. In *Modern Carbonylation Methods*; Kollár, L., Ed.; Wiley-VCH: Weinheim, 2008; pp 27−64.

the first indication that molecular $Ni^{II}\cdots Fe^{II}$ sites and bridges can be constructed. Any further elaboration of these binuclear systems should include reduced intermetal separation to <∼3.0 Å as in the C-cluster (Figure 1), which might prove advantageous for bridged hydroxycarbonyl formation from a CO reaction and unidentate linear or bent cyanide ligation. Ultimately, the bridging unit should be integrated into a $Fe\cdots NiFe_3S_4$ bridged assembly, a future goal.

(51) While reaction of CO with reduced Ni complexes remains a possibility, preliminary investigation of **1** (DMF) and **7** (acetonitrile) by cyclic voltammetry reveals only quasi-reversible reductions at−1.40 and−1.31 V, respectively, vs SCE. Both complexes showed reversible oxidations (**1**, +0.67 V; **7**, +1.04 V).

**Acknowledgment.** This research was supported by NIH Grant GM No. 28856. We thank Dr. S.-L. Zheng for assistance with crystallography.

**Supporting Information Available:** Crystallographic data for the 15 compounds in Tables S1−S3 and structures of compounds **2**−**4**, **20**, and **21** in Figure S1. This material is available free of charge via the Internet at http://pubs.acs.org.

JA1003125